=== **SEMICONDUCTORS** ===

Magnetic States of Fe^{2+} Ions in $Fe_xMn_{1-x}S$ Induced by Chemical Pressure

G. M. Abramova^{a,}*, Yu. V. Knyazev^a, O. A. Bayukov^a, and S. P. Kubrin^b

^{a} *Kirensky Institute of Physics, Federal Research Center KSC, Siberian Branch Russian Academy of Sciences, Krasnoyarsk, 660036 Russia*

^{b} *Research Institute of Physics, Southern Federal University, Rostov-on-Don, 344090 Russia*

**e-mail: agm@iph.krasn.ru*

Abstract—Influence of the chemical pressure (x) in single crystals of $Fe_xMn_{1-x}S$ ($0.12 \le x \le 0.29$) on the spin state of iron ions was studied by Mössbauer spectroscopy in the temperature range from 4.2 to 300 K. Peculiarities of formation of the paramagnetic and antiferromagnetic phases of solid solutions were found. Substitution of Fe^{2+} cations in the high-spin state for Mn^{2+} was found to occur in $Fe_xMn_{1-x}S$ as x changes. A decrease in the distance between the ions in $Fe_xMn_{1-x}S$ induces changes in the state of the Fe^{2+} ions in the samples with $x = 0.25$ and 0.29. The asymmetry parameter of the electric field gradient (EFG) tensor and the angle between the directions of the magnetic moment and the principal axis of the electric field gradient were found to change in the magnetically ordered phase at 4.2 K; the angle between the magnetic moment and the electric field gradient axis changes from 21° in the sample with $x = 0.12$ to 33° when $x = 0.29$.

INTRODUCTION

Cubic semiconductor α-MnS belongs to the group of strongly correlated compounds of the MnO type [1]. This sulfide shows an insulator–metal transition [3] accompanied by the structural rearrangement with changing lattice symmetry at 26–30 GPa and by spin crossover [4]. The spin state of Mn^{2+} ions is changed continuously in the pressure range from 10 to 40 GPa [4]. The mechanism of spin crossover in the strongly correlated compounds (of the MnO type) was explained in [1, 2] through a change in the conductivity type.

Compounds synthesized based on manganese monosulfide α-MnS are presented in [5]. It was found that as the degree of cationic substitution in sulfides $Fe_xMn_{1-x}S$ increases ($0 \le x \le 0.29$), the critical hydrostatic pressure of the insulator–metal transition decreases so that the compounds with $0.25 \le x \le 0.29$ are semimetals at the atmospheric pressure. As x grows, the Neel temperature T_N for $Fe_xMn_{1-x}S$ grows from 147–156 K in α-MnS [6, 7] to 205 K at $x = 0.29$ [8]. The Néel temperature shifts to 280 K and the magnetization of the compound decreases under the hydrostatic pressure of 4 GPa [9]. Since the chemical pressure arising when the degree of cationic substitution in crystal changes is, in a sense, analogous to the hydrostatic pressure, the studies of the magnetic state

of 3d ions in solid solutions based on α-MnS and the question if the spin crossover induced by changes in x is possible under the atmospheric pressure are of interest.

The present work reports the results of studies of the solid solution in the system $Fe_xMn_{1-x}S$ ($0.12 \le x \le 0.29$) by ^{57}Fe Mössbauer spectroscopy in the temperature range of 4.2–300 K, aimed at revealing the spin state of the Fe^{2+} ions with varied values of the cationic substitution, temperature, and magnetic ordering.

EXPERIMENTAL

Solid solutions $Fe_xMn_{1-x}S$ ($0.12 \le x \le 0.29$) were obtained as described in [10]. Initial compounds ($x = 0.12, 0.18, 0.25$, and 0.29) were single crystals of $Fe_xMn_{1-x}S$ with the FCC NaCl-type structure; compositions corresponded to the given value of x with the accuracy of ±0.02, which was proved by X-ray and energy dispersive spectroscopy [5, 8, 10]. Samples for Mössbauer studies were prepared by grinding the crystals (the thickness of 5–10 mg/cm² with respect to the natural iron content). Mössbauer spectra were obtained in the temperature range of 4.2–300 K on the MS-1104Em spectrometer in the transmission geometry using the ^{57}Co (Rh) source and a helium cryostat. The spectra were processes in two steps. First, proba-
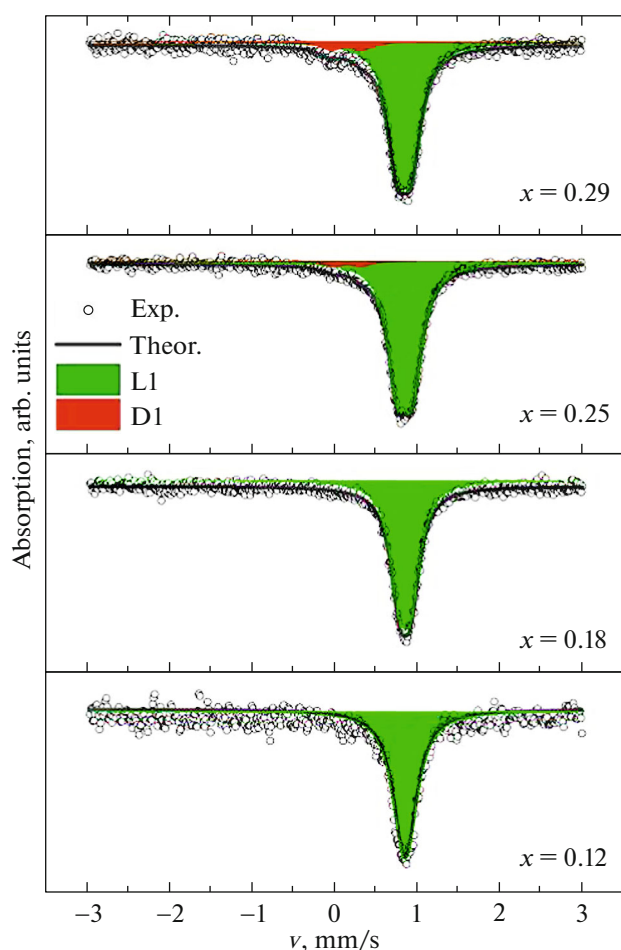
Fig. 1. Mössbauer spectra of $Fe_xMn_{1-x}S$ ($0.12 \le x \le 0.29$) at room temperature. Circles represent experimental data; solid lines, theoretical spectra. Singlet (L1) and doublet (D1) are highlighted.

Fig. 2. Quadrupolar splitting probabilities for the main singlet (high spin) and the additional doublet (low spin) of Fe^{2+} in $Fe_xMn_{1-x}S$ ($0.12 \le x \le 0.29$) at 300 K.

bility distributions of the quadrupolar splitting $P(\text{QS})$ in the experimental spectra were calculated. Possible nonequivalent crystallographic positions of iron were determined based on these results. In the second step, preliminary spectra were built and then fitted to the experimental data by varying the whole set of hyperfine parameters using the linear approximation of the mean square minimization method [11]. The spectra obtained at 4.2 K were processed in the SpectrRelax program [12] using the full Hamiltonian, allowing for magnetic dipolar and quadrupolar interactions. Chemical shifts are determined relative to α-Fe.

RESULTS AND DISCUSSION

According to X-ray analysis [5, 10], cationic substitution in $Fe_xMn_{1-x}S$ at room temperature ($0 \le x \le 0.29$) is accompanied by a decrease in the unit cell parameter from 5.224 Å (at $x = 0$) to 5.165 Å (at $x = 0.29$) with the cubic symmetry of the lattice remaining
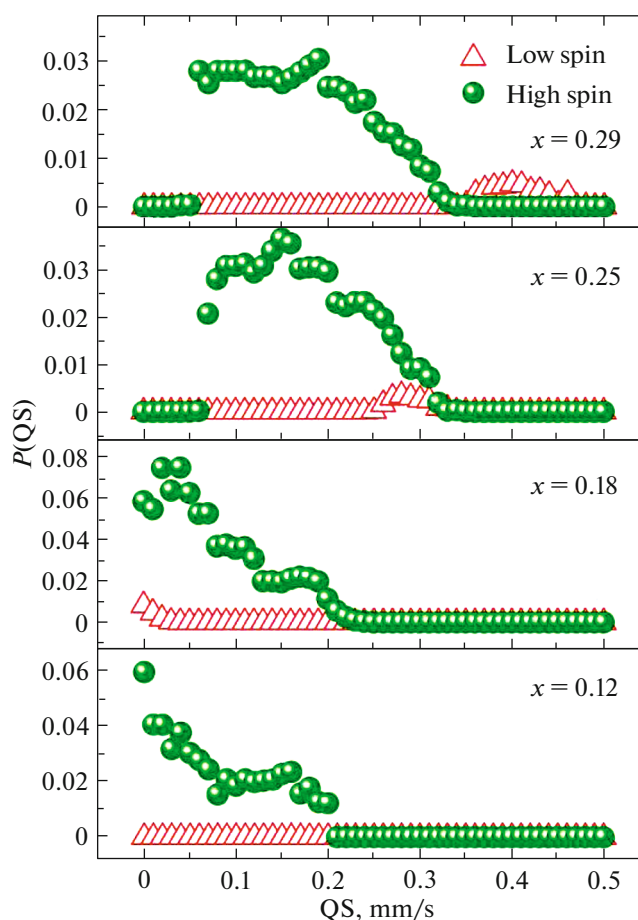
intact (space group *Fm*-3*m*). Mössbauer spectra of $Fe_xMn_{1-x}S$ ($0.12 \le x \le 0.29$) at 300 K are shown in Fig. 1. The main component in the spectra of the samples with $x = 0.12$ and 0.18 at 300 K is a singlet, which is also evident from the distribution $P(\text{QS})$ in Fig. 2. The parameters of the main singlet line in the spectra of these samples correspond to the bivalent ion Fe^{2+} in the high-spin (HS) state having the electron configuration d^6, ($^4t_{2g}^2e_g$); this gives the evidence of isovalent substitution for spherically symmetrical Mn^{2+} ions (electron configuration d^5, $^3t_{2g}^2e_g$) in the solid solutions. As the cationic substitution degree grows at $x > 0.18$, the singlet is broadened due to appearance of an additional quadrupolar splitting compared with the linewidth of Mössbauer absorption, which is in agreement with the results of [10]. The chemical shift IS of the main peak decreases as x grows in $Fe_xMn_{1-x}S$ (Fig. 3, curve IS) and correlates with the decrease in the cubic lattice parameter (Fig. 3, curve *a*), which is an indirect evidence of the increase in the chemical pressure in the crystals. A similar behavior of IS was
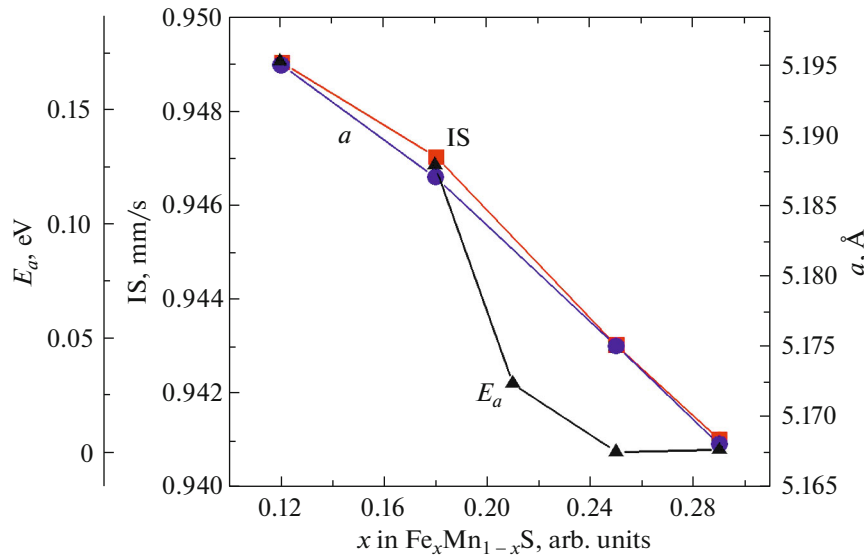
Fig. 3. Concentration dependence of the chemical shift IS of the main components of the spectrum; lattice parameter a, and the activation energy of conduction E_a in the paramagnetic state of the $Fe_xMn_{1-x}S$ samples ($0.12 \leq x \leq 0.29$).

observed, for example, in (Mg,Fe)O under hydrostatic pressure [13]. A distinct enough correlation of the chemical shift IS of the main line in the spectra and the lattice parameter with the sulfide composition in $Fe_xMn_{1-x}S$ ($0.12 \leq x \leq 0.29$) (Fig. 3) shows that the decrease in IS with increasing x is caused by growing electron density on the ^{57}Fe nuclei due to decreased interatomic distances. Allowing for the high symmetry of the cubic lattices (FCC, NaCl, sp. gr. Fm-$3m$) of solid solutions $Fe_xMn_{1-x}S$ ($0.12 \leq x \leq 0.29$), the electron levels e_g and t_{2g} of Mn^{2+} ions should remain degenerate. However, Fe^{2+} ion may distort the symmetrical octahedral environment due to the Jahn–Teller effect, and quadrupolar splitting should appear in the Mössbauer spectrum, like it was observed for isostructural FeO [14]. Experimental data for the samples of $Fe_xMn_{1-x}S$ reveal only broadening of the main spectral peak due to weak quadrupolar splitting QS (~0.18 mm/s). To explain this fact, we can suppose that competing spin-orbital and Jahn–Teller contributions take place in the studied compounds. The high-spin cation Fe^{2+} possesses a nonzero magnetic moment [15], and hence it is reasonable to expect that it will show spin-orbital interaction competing with the splitting of the t_{2g} levels caused by the Jahn–Teller effect [16]. The Jahn–Teller contribution tends to release the degeneracy of the t_{2g} levels, while the spin-orbital interaction tends to save it. As a result of this competition, only weak quadrupolar splitting of the main peak in the experimental spectra of the paramagnetic state of $Fe_xMn_{1-x}S$ samples is observed, which corresponds to the HS Fe^{2+}.

Figure 3 shows that the lattice compression for the samples of $Fe_xMn_{1-x}S$ with $x > 0.18$ is accompanied by a sharp decrease in the activation energy of conduction in the paramagnetic state of the studied compounds. Appearing of the metal phase in the compositions with $x \sim 0.25$ is proved by optical studies [17]. Figures 1 and 2 show an additional doublet, which appears in the left part of the Mössbauer spectra of the samples with $x > 0.18$ and becomes more intensive as x grows. The chemical shift of this additional doublet at 300 K is 0.23 ± 0.01 mm/s for both samples, and the quadrupolar splitting changes from 0.33 mm/s for $x = 0.25$ to 0.39 mm/s for $x = 0.29$. These values of IS and QS are typical of the low-spin (LS) state of the Fe^{2+} ion and are observed in the vicinity of spin crossover, for example, in the (Mg,Fe)O system [13] and FeS [18]. Since the cation LS Fe^{2+} with the electron configuration t_{2g}^6 has zero spin and hence does not experience spin-orbital interaction and Jahn–Teller effect, it becomes spherically symmetrical as Mn^{2+}. Similar to the manganese ion, it can experience the influence of the cubic field and the temperature [13]. Another possible reason for appearing of the new doublet may be formation of Fe^{3+} ions in strong covalent bonds Fe–S. Parameters typical for Fe^{3+} ions in isostructural compounds are IS ~ 0.55 mm/s and QS ~ 0.90 mm/s [13, 19], which differ from the parameters of the doublet observed in $Fe_xMn_{1-x}S$ ($0.25 \leq x \leq 0.29$). At the same time, experimental values of the quadrupolar splitting (0.33 mm/s for $x = 0.25$ and 0.39 mm/s for $x = 0.29$) are close to the observed and calculated values for LS Fe^{2+} (QA = 0.4 mm/s) obtained in [13] for isostructural compounds (Mg,Fe)O. Author suggests that the mechanism of appearing of weak quadrupolar splitting is related to the thermal effect and distortion of the FeO_6 octahedron. In the case of LS Fe^{2+} this distor-
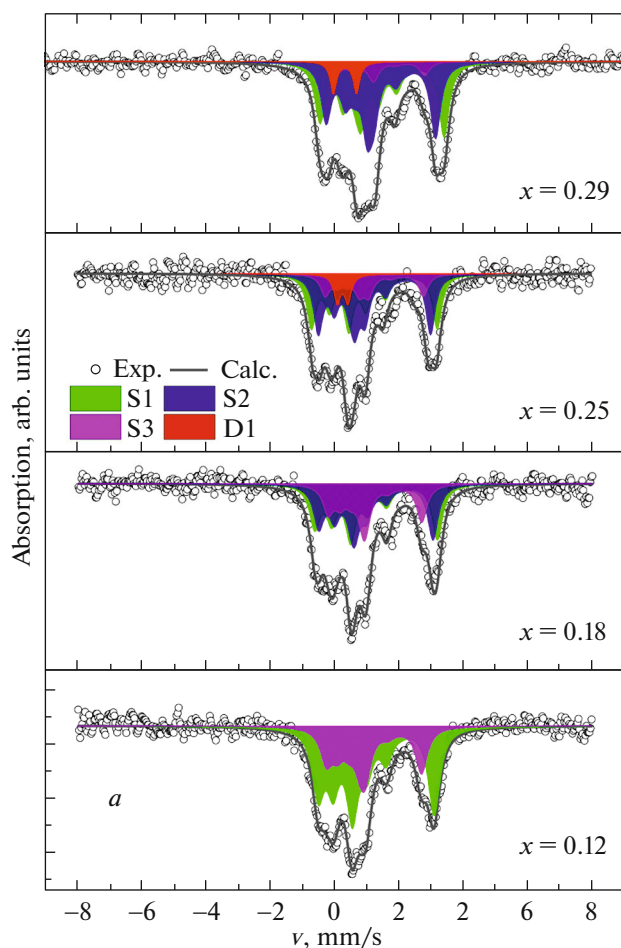
Fig. 4. Mössbauer spectra of Fe$_x$Mn$_{1-x}$S ($0.12 \leq x \leq 0.29$) at 4.2 K. Circles represent experimental data; solid lines, theoretical spectra. The states HS Fe^{2+} (S1, S2, S3) and the doublet (D1) are highlighted.

Fig. 5. Probability distributions of the hyperfine field H in sulfides Fe$_x$Mn$_{1-x}$S ($0.12 \leq x \leq 0.29$) at 4.2 K.

tion is stronger than for HS Fe^{2+}, but the electric field gradient is small because the main contribution into the EFG belongs to the valence electrons rather than the lattice.

Mössbauer studies for the Fe$_x$Mn$_{1-x}$S samples ($0.25 \leq x \leq 0.29$) in the magnetically ordered state were carried out at the temperatures of 4.2, 110, and 140 K. Spectra measured at 110 and 140 K are similar to those observed for α-MnS [6]. Transition into the magnetically ordered state of Fe$_x$Mn$_{1-x}$S is accompanied by an increase in the chemical shift and quadrupolar splitting of the main spectral line, and also by appearing of nonzero hyperfine magnetic field H. At the same time, the additional doublet retains its nonmagnetic character.

Figure 4 shows Mössbauer spectra of the Fe$_x$Mn$_{1-x}$S samples ($0.12 \leq x \leq 0.29$) in the magnetically ordered state at 4.2 K. Magnetic and electric nuclear interactions at 4.2 K become comparable, and hence two for-
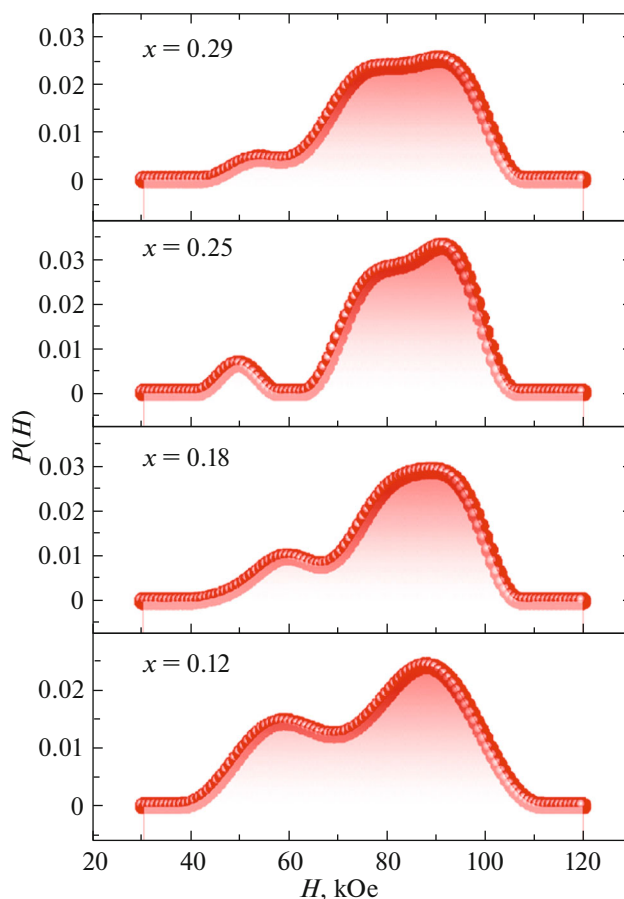
bidden nuclear transitions of ^{57}Fe with $\Delta m = \pm 2$ become possible. Analysis of the full Hamiltonian in the SpectrRelax program allowed calculating the angles between the hyperfine field H and the EFG. The hyperfine parameters of the Fe$_x$Mn$_{1-x}$S samples at 4.2 K are listed in the Table 1. Evidently, the chemical shift IS and quadrupolar shift QS for the high-spin Fe^{2+} ions increase in the low-temperature antiferromagnetic phase of Fe$_x$Mn$_{1-x}$ ($0.12 \leq x \leq 0.29$) as compared with the paramagnetic phase. According to [6, 7], the value of the chemical shift extrapolated to 0 K is 1.12 mm/s for α-MnS, while for the isostructural but more covalent compound MnSe IS = 1.06 mm/s. The low-temperature values of IS for Fe$_x$Mn$_{1-x}$S are closer to the covalent selenide MnSe. Paper [7] reports two characteristic states of ^{57}Fe−α-MnS (NaCl) at 5 K, in which the hyperfine magnetic field H takes the values of 51.9 and 49.5 kOe, and corresponding quadrupolar splittings are −1.2 and −1.38 mm/s. Experimental values of quadrupolar shift QS for Fe$_x$Mn$_{1-x}$S (see Table 1) are typical of high-spin Fe^{2+} ions in distorted octahedra [13].

Table 1. Mössbauer parameters of $Fe_xMn_{1-x}S$ ($0.12 \leq x \leq 0.29$) at 4.2 K

Parameter	IS, ±0.005 mm/s	QS, ±0.01 mm/s	H, ±5 kOe	θ, ±2°	η	G, ±0.01 mm/s	A, ±3%
			$x = 0.12$				
S1	1.032	2.83	56	22	0.66	0.44	33
S2	1.023	2.57	87	22		0.44	67
			$x = 0.18$				
S1	1.045	2.70	59	22	0.62	0.40	26
S2	1.005	2.78	84	22		0.40	37
S3	0.985	2.67	94	22		0.40	37
			$x = 0.25$				
S1	1.070	3.08	58	24	0.54	0.36	16
S2	1.010	2.73	81	24		0.36	41
S3	0.970	2.80	95	24		0.36	37
D1	0.244	0.17	—	—	—	0.25	6
			$x = 0.29$				
S1	1.061	2.57	55	33	0.34	0.39	8
S2	1.041	2.89	75	33		0.39	44
S3	1.021	2.84	93	33		0.39	43
D1	0.340	0.35	—	—	—	0.25	6

IS is the isomeric chemical shift relative to α-Fe; QS is the quadrupolar shift; H is the hyperfine field at the iron nucleus; θ is the polar angle of H with respect to the EFG; η is the EFG asymmetry parameter; G is the Mössbauer line width at half-height; A is the relative fraction in the spectrum.

Distributions of hyperfine fields H for $Fe_xMn_{1-x}S$ ($0.12 \leq x \leq 0.29$) at 4.2 K are plotted in Fig. 5. Maxima on the distribution curves $P(H)$ show that as x grows, three magnetically nonequivalent states appear for high-spin Fe^{2+} ions with different characteristic hyperfine fields H. A similar phenomenon was observed in α-MnS enriched with the ^{57}Fe isotope [20]. Estimating the probability of random distribution of iron cations in the structure of $Fe_xMn_{1-x}S$ showed that at $x = 0.12$ there is a significant probability of one Fe^{2+} cation appearing among its closest neighbors. As the substitution level increases to $x = 0.29$, the probability of existing of larger number of neighbor Fe^{2+} cations grows, which is reflected in the Mössbauer spectra. Apparently, the concentration inhomogeneity of the distribution of Fe^{2+} cations over the volume of the $Fe_xMn_{1-x}S$ solid solution leads to appearance of additional nonequivalent magnetic states of iron Fe^{2+} in the samples, which agrees with the neutron studies [7].

It is known that α-MnS at 20 K has the antiferromagnetic structure with the magnetic moments of Mn^{2+} ions oriented along the [110] axis of the cubic lattice [21]; the EFG orientation corresponds to one of the cube diagonals [111] and is related to a weak rhombohedral distortion of the cubic lattice of the monosulfide [6, 7, 22]. According to the experimental data (see Table 1), the polar angle θ between the hyperfine field direction and the EFG axis grows from 21° at $x = 0.12$ to 33° at $x = 0.29$ in $Fe_xMn_{1-x}S$ solid solutions. At the same time the asymmetry parameter η of the EFG tensor also changes, which points to a change in the lattice symmetry of $Fe_xMn_{1-x}S$ as the substitution degree is varied.

It follows from Table 1 that the additional doublet is present in the spectra of the magnetically ordered phase of $Fe_xMn_{1-x}S$ with $x = 0.25$ and 0.29, and it is nonmagnetic till 4.2 K. As the temperature decreases, the quadrupolar splitting of the doublet also decreases, but this effect is within the experimental error. Still it is worth noting that the specific resistance of the samples with $x = 0.25$ and 0.29 at temperatures of 4.2–77 K is several orders of magnitude lower than that of the compositions with $x = 0.12$ and 0.18 [5]. Thus, appearance of nonmagnetic states of iron ions with low values of IS and QS (the new doublet) in the solid solutions with $x = 0.25$ and 0.29 may be related to the change in the conductivity type caused by the chemical pressure. Appearance of states of this kind explains also the increase in magnetization revealed by neutron diffractometry under the hydrostatic pressure of 4.2 GPa in $Fe_xMn_{1-x}S$ samples with $x = 0.27$ [9].

The phenomenon of spin crossover becomes possible if $10Dq > 2.5B + 4C$, where B and C are the Racah parameters which for the Fe^{2+} ion in the cubic structure are 1040 and 3809 cm^{-1}, respectively [23]. Then

the necessary splitting is 17836 cm^{-1}, or 2.07 eV. The value of $10Dq$ for manganese monosulfide with the FCC structure (defining the energy difference between the e_g and t_{2g} states of a $3d$ ion) at 300 K is 0.9 eV [24]; it grows to 1.26 eV at 4.2 K [25], and the volume of the unit cell of the cubic lattice at the same time changes by about 2%. The unit cell volume of the solid solution of Fe$_x$Mn$_{1-x}$S ($0.12 \leq x \leq 0.29$) at room temperature decreases by almost 4% compared with $x = 0$ (α-MnS) as x increases. Therefore, one can expect that $10Dq$ attains significant local values. For instance, this parameter achieves the value of 2 eV for octahedral positions of Fe^{2+} in FeS under the pressure of $5-7$ GPa [18].

Allowing for everything stated above, it is possible that the found peculiarities of the Mössbauer spectra of the Fe$_x$Mn$_{1-x}$S samples with $x = 0.25$ and 0.29 may be due to the coexistence of the HS and LS states of $3d$ ions, which appear due to an increase in the cubic field in locally distorted locations in the crystal. Appearance of Fe^{2+} ions with low values of IS and QS may be caused by formation of a short-range order, preceding structural transformation occurring upon lattice compression. However, additional Mössbauer studies of Fe$_x$Mn$_{1-x}$S under hydrostatic pressure are needed to substantiate this hypothesis.

CONCLUSIONS

Mössbauer spectra of Fe$_x$Mn$_{1-x}$S samples with $0.12 \leq x \leq 0.29$ measured in the temperature range from 4.2 to 300 K were studied. Fe^{2+} ions were found to have a high-spin state in locally distorted octahedral positions of the solid solution. As the substitution degree grows in the paramagnetic state, the chemical shift decreases and a weak quadrupolar splitting of the main spectral line appears. In the samples with $0.25 \leq x \leq 0.29$, the chemical pressure leads to appearing of new Fe^{2+} states corresponding to the additional doublet with the IS value typical of LS Fe^{2+}. In the magnetically ordered phase of the sulfides Fe$_x$Mn$_{1-x}$S ($0.12 \leq x \leq 0.29$), structural disorder increases as x grows, and this leads to formation of nonequivalent states with different values of the quadrupolar shift ($\sim 2.5-3.0$ mm/s) and hyperfine magnetic field ($\sim 56-95$ kOe). Increasing chemical pressure causes rotation of the magnetic moment, which is evidenced by the change in the polar angle θ between the hyperfine magnetic field vector and the EFG axis from 21° for $x = 0.12$ to 33° for $x = 0.29$. This is accompanied also by the change in the asymmetry parameter, which means that the symmetry of the lattice in the antiferromagnetic state is altered. The additional doublet in the semimetal samples with $0.25 \leq x \leq 0.29$ is nonmagnetic in the whole studied temperature range. Obtained results allow suggesting that Mössbauer studies of sulfides Fe$_x$Mn$_{1-x}$S ($0.12 \leq x \leq 0.29$) under hydrostatic pressure are promising to understand the nature of the Fe^{2+} ion states.

CONFLICT OF INTEREST

The authors declare that they have no conflicts of interest.

REFERENCES

1. J. Kunes, A. V. Lukoyanov, V. I. Anisimov, R. T. Scalettar, and W. E. Pickett, Nat. Mater. **7**, 198 (2008).

2. S. G. Ovchinnikov, JETP Lett. **94**, 192 (2011).

3. Y. Mita, M. Kobayashi, S. Endo, and S. Mochizuki, J. Magn. Magn. Mater. **272–276**, 428 (2004).

4. Y. Wang, L. Bai, T. Wen, L. Yang, H. Gou, Y. Xiao, P. Chow, M. Pravica, W. Yang, and Y. Zhao, Angew. Chem. Int. Ed. **55**, 10350 (2016).

5. G. M. Abramova, A. Hanzawa, T. Kagayama, Y. Mita, E. M. Eremin, G. M. Zeer, S. M. Zharkov, and S. G. Ovchinnikov, J. Magn. Magn. Mater. **465**, 775 (2018).

6. R. J. Pollard, V. H. McCann, and J. B. Ward, J. Phys. C **16**, 345 (1983).

7. R. J. Pollard, *Mössbauer Spectroscopy of Some Magnetic Materials* (Univ. of Canterbury, 1982).

8. G. Abramova, J. Schefer, N. Aliouane, M. Boehm, G. Petrakovskiy, A. Vorotynov, M. Gorev, A. Bovina, and V. Sokolov, J. Alloys Compd. **632**, 562 (2015).

9. G. Abramova, M. Boehm, J. Schefer, A. Piovano, G. Zeer, S. Zharkov, Y. Mita, and V. Sokolov, JETP Lett. **106**, 498 (2017).

10. G. Abramova, N. Volkov, G. Petrakovskiy, V. Sokolov, M. Boehm, O. Bayukov, A. Vorotynov, A. Bovina, and A. Pischjugin, J. Magn. Magn. Mater. **320**, 3261 (2008).

11. Yu. V. Knyazev, A. S. Tarasov, M. S. Platunov, A. L. Trigub, O. A. Bayukov, A. I. Boronin, L. A. Solovyov, E. V. Rabchevskii, N. N. Shishkina, and A. G. Anshits, J. Alloys Compd. **820**, 153073 (2020).

12. M. E. Matsnev and V. S. Rusakov, AIP Conf. Proc. **1489**, 178 (2012).

13. I. Kantor, L. Dubrovinsky, C. McCammon, G. Steinle-Neumann, A. Kantor, N. Skorodumova, S. Pascarelli, and G. Aquilanti, Phys. Rev. B **80**, 014204 (2009).

14. C. A. McCammon and D. C. Price, Phys. Chem. Miner. C **250**, 254 (1985).

15. R. J. Radwanski and Z. Ropka, arXiv:cond-mat/0010032v1 [condmat. str-el] (2000).

16. F. J. Berry, *Chemical Bonding and Spectroscopy in Mineral Chemistry* (Chapman and Hall, London, New York, 1985).

17. G. M. Abramova, N. V. Volkov, G. A. Petrakovskioe, Y. Mita, O. A. Bayukov, D. A. Velikanov, A. M. Vorotynov, V. V. Sokolov, and A. F. Bovina, JETP Lett. **86**, 371 (2007).

18. Z. Ropka and R. J. Radwanski, Phys. Status Solidi A **196**, 275 (2003). https://doi.org/10.1002/pssa.200306405

19. L. Aldon and J.-C. Jumas, Solid State Sci. **14**, 354 (2012).

20. A. Tomas, L. Brossard, J. L. Dormann, and M. Guittard, J. Magn. Magn. Mater. **31**, 755 (1983).

21. S. Steger and V. Yu. Pomjakushin, VP Report (2008).

22. H. van der Heide, C. F. van Bruggen, G. A. Wiegers, and C. Haas, J. Phys. C **16**, 855 (1983).

23. S. Ivascu, A. S. Gruia, and N. M. Avram, Phys. B (Amsterdam, Neth.) **450**, 146 (2014). https://doi.org/10.1016/j.physb.2014.05.065

24. M. Kobayashi, T. Nakai, S. Mochizuki, and N. Takayama, J. Phys. Chem. Solids **56**, 341 (1995).

25. H. Komura, J. Phys. Soc. Jpn. **26**, 1446 (1969).

Translated by S. Efimov